Low Scaling Second-order Møller–Plesset Perturbation Methods for Electron Correlation

Si Chen
Supervisor: Prof. Ria Broer, dr. Remco Havenith
Zernike Institute of Advanced Materials, University of Groningen, The Netherlands

Abstract

Nowadays, more and more efforts have been paid to the study of nanosystems from not only technological aspects but also theoretical aspects. And theoretically, electron correlation is an important aspect to make the theoretical calculation more accurate and useful. However, to study nanosystems while accounting for the electron correlation, one needs to tackle the steep power law dependence of computing time on the molecular size. Despite solving this problem by improving the computer technology, new methods should be introduced to lower the steep scaling. In this paper, we focus on the so-called local Møller–Plesset perturbation theory (LMP2) methods. Three specific methods will be discussed here, that is, the original Pulay methods, atomic orbital Laplace LMP2 methods, and density fitting LMP2 methods. Then applications using LMP2 methods will be discussed. One is using the LMP2 method to study DNA systems: it took 49.5 days to calculate a DNA system containing 1052 atoms by the LMP2 method, while it would take two years by conventional MP2. The second is that LMP2 methods have been incorporated into the CRYSCOR program for periodic systems. The efficiency of the program is illustrated for 1D-, 2D-, 3D- systems respectively in this paper. In particular, the rolling energy of a boron nitride nanoscroll, the adsorption of an argon monolayer on the MgO (100) surface, and the relative stability of different aluminosilicates are discussed. In the last application, the LMP2 method was applied to study the cohesive energy of the CO_2 crystal and it leads to an accurate and inexpensive calculation. For the future development of the LMP2 method, a few suggestions will be made at the end of this paper.

Content

Abstract 1
1. Introduction 2
2. Theory 3
2.1 Pulay-Saebø method 3
2.2 Atomic orbital Laplace MP2 methods 5
2.3 Density fitting LMP2 7
2.4 Discussion 9
3. Applications 10
3.1 DNA systems 10
3.2 CRYSCOR: a program for 1D-, 2D- and 3D-periodic systems 11
3.3 Cohesive Energy of Molecular Crystals 14
4. Discussion and suggestions for future work 18
5. Reference 19

1. Introduction

Appealed by the interesting properties of nanosystems, computational chemists have paid a lot of efforts to study those systems by means of ab initio calculations. As the classical Hartree-Fock (HF) mean-field approach to the Schrödinger equation did not take electron-correlation effects into account, two ways to correct this error were introduced, that is, Density Functional Theory (DFT) methods and wavefunction-based correlation methods. However, for such large system, computational time and storage space of those methods become the bottleneck. Conventional DFT methods scale formally as $O(N^4)$ and the least expensive one of the wavefunction-based correlation methods, *viz.,* the second-order Møller–Plesset perturbation method (MP2), scales formally as $O(N^5)$. In this case, people try to lower the scaling for calculation.

For DFT, people have tried to use techniques such as the fast multipole method (FMM), fast quadrature, and alternatives to diagonalization like conjugate gradient density matrix search (CGDMS), to linearize the DFT method. But DFT has some limitations: the self-repulsion and self-correlation of electrons, or the lack of long-range van der Waals dispersion, as well as no systematic way to estimate or improve the quality of the results, which lead people turn to wavefunction-based correlation methods.

Fortunately, for wavefunction-based correlation methods, such high scaling is unphysical and low scaling can be reached by local correlated methods. Local correlated methods were introduced in the 1980s by Pulay.[1-3] Most of the work on low scaling correlation methods has focused on the less expensive correlation method, MP2. However, Scuseria and Ayala also have successfully applied local correlated method to coupled-cluster doubles (CCD), and the Stuttgart group have managed to use that for more accurate correlation methods including coupled cluster singles and doubles with and without approximate triples correction, i.e. LCCSD and LCCSD(T).[4]

In this paper, we will focus on LMP2. Although MP2 is not as accurate as CCSD, it is popular due to its simplicity and low cost, and by far it is the only way to make good estimations of the properties of very large systems. What is more, the research on low scaling MP2 can also act as a stepping stone for low scaling more accurate methods.

Based on Pulay's local correlated method, a lot of schemes were brought up to realize low scaling of MP2. The Stuttgart group used pre-selected local domains in the spirit of Pulay local correlation method.[5] The Rice group employed Almlof and Häser's Laplace transform method to eliminate the MP2 energy denominators.[6] The Columbia group applied a pseudospectral formulation for generation of the electron repulsion integrals in MO basis.[7] The Berkeley group's method is based on a tensor formulation of electron correlation. In recent years, density fitting was also introduced in local correlation methods,[8] which improves the efficiency for the calculation of extended molecular systems considerably.

The organization of this article is as following: Section 2 will cover efforts paid towards low scaling MP2 in a theoretical manner with emphasize on the original Pulay method[1], atomic orbital Laplace MP2 method[6], and density fitting local MP2 method[8]. Then in Section 3, three applications using LMP2 will be discussed. Firstly, the LMP2 method will be used to study the DNA system. Secondly, a program called CRYSCOR, which uses LMP2 method, will be discussed. In the third application, the cohesive energy of CO_2 will be studied by the LMP2 method. In the end, conclusions and suggestions for LMP2 will be made in Section 4. And in this paper, the emphasis is on the theory instead of implementation.

2. Theory

2.1 Pulay-Saebø method

For simplicity, only the closed-shell case is considered here.

The main idea of the Pulay-Saebø local correlated method is omitting unimportant configurations by using localized orbitals. Specifically, two strategies are used: for occupied orbitals, they use molecular orbitals, which are typically localized by Boys localization[9]; for virtual orbitals, they use atomic basis functions projected against the self-consistent field (SCF) orbitals.

One problem of using localized orbitals in second-order Møller–Plesset perturbation theory is that MP2 is formulated in terms of canonical orbitals. In the spin-adapted generator state formalism[10], the MP2 energy expression is:

$$E_{MP2} = -\sum_{i \geq j}(2-\delta_{ij})\sum_{a,b}(\mathrm{K}_{ij})^{ab}\left\{2(\mathrm{K}_{ij})^{ab} - (\mathrm{K}_{ji})^{ab}\right\} / (\varepsilon_i + \varepsilon_j - \varepsilon_a - \varepsilon_b) \tag{1}$$

Where i, j, k… are used for internal orbitals and a, b, c… for virtual orbitals, the Greek letters μ, ν, λ are used for atomic orbitals (AO), and this convention will be used throughout the paper.

The ε's are orbital energies, and (K_{ij}) is the internal exchange matrix for pair (i, j). The (a,b) element of this matrix is the transformed integral:

$$(\mathrm{K}_{ij})^{ab} = (i,a \mid j,b) \equiv \iint i(1)a(1)\frac{1}{r_{12}}j(2)b(2)d\tau_1 d\tau_2 \tag{2}$$

To address this problem, they introduced an orbital invariant formulation of Møller–Plesset perturbation theory[1,11,12]. In the generator state formulism the pair amplitudes, collected in matrices T_{ij}, are determined from the equation:

$$K_{ij} + FT_{ij}S + ST_{ij}F - \sum_k S(f_{ik}T_{kj} + f_{kj}T_{ik})S = 0 \tag{3}$$

Where F is the Fock-matrix, S is the overlap matrix and f_{ik} are the non-diagonal Fock matrix elements. All matrices above represented with capital letters are defined in a projected AO basis (p,q). To illustrate the projection of matrices, take the internal exchange matrix for example:

$$(\mathrm{K}_{ij})^{p,q} = (i,p \mid j,q) = \sum_{\mu,\lambda}(P)^{\mu,p}(\mathrm{K}_{ij})^{\mu,\lambda}(P)^{\lambda,q} \tag{4}$$

The projection matrix P is defined by $P = I - \frac{1}{2}DS$, where I is the unit matrix, D is the doubly-occupied density matrix and S is the overlap matrix, both in the unprojected AO basis (μ, ν). The MP2 energy can be calculated from the formula:

$$E_{MP2} = -\sum_{i \geq j}(2-\delta_{ij})\sum_{p,q}(\mathrm{K}_{ij})^{p,q}\left\{2(T_{ij})^{p,q} - (T_{ji})^{p,q}\right\} \tag{5}$$

Equation 5 produces the same result as Equation 1 which uses a canonical formulation.

2.1.1 Treatment of weak pairs and distant pairs

As in the localized formulism, the correlation energy between electron pairs decreases rapidly with distance d between orbital pairs ($\propto 1/d^6$), which is defined as the distance between the centers of the two localized orbitals, linear scaling will be realized if criteria is made to screen some pairs according to their correlation strength. To implement this idea, pairs are classified into four categories: significant pairs, weak pairs, distant pairs and negligible pairs by estimating the pair correlation energy in terms of the London dispersion formula[4]:

$$E_{ij}^{\ est} \approx C r_i^3 r_j^3 / d^6 \tag{6}$$

Where C is a constant, related to the HOMO-LUMO gap, r_i is the radius of the localized orbital, which represents the degree of localization, and d is the distance between the centers of the two localized orbitals. To improve efficiency, different strategies should be adopted to calculate different kinds of pairs. Negligible pairs are dropped from the calculation. For distant pairs, they are successfully approximated by Pulay and the Stuttgart group utilizing a multipole expansion[13]. For weak pairs, Saebø et al. used a basis of pseudonatural orbitals[14] (or pair natural orbitals). The linear scaling is thus realized, as the number of weak and negligible pairs increases roughly as N^2, while the number of significant pairs increases only linear with N.

2.1.2 Truncation of virtual space

The virtual space expands steeply and unphysically with N, whereas only the virtual orbitals that are spatially close to a given pair of occupied orbitals contribute significantly to the pair correlation. Besides, virtual orbitals are more difficult to localize than occupied orbitals. Thus Pulay truncated the virtual space by using a local virtual basis set. And to ensure the orthogonality between virtual and occupied subspaces, AOs are projected onto the virtual space. The truncation is realized by assigning a subset of AOs, i.e. domain D(i), to each correlated occupied orbital |i>.

Another advantage of the truncation of the virtual space besides saving in computational cost according to Saebø et al.[15] is that it also avoids the basis set superposition artifact. They argued that the canonical method suffers from this problem because of basis set incompleteness, which affects the pair correlation energy caused by delocalization of correlated pairs. However, if a local basis is used, the pair correlation energy stays almost constant as a function of the size of system.

2.1.3 Improvements to old Pulay methods

Based on the original Pulay method, several improvements to both scaling and accuracy have been proposed.

2.1.3.1 Prescreening of AO integrals

Linear scaling in terms of calculation of integrals in AO basis can be achieved by a prescreening procedure based on an estimate of an integral's contribution to half-transformed integrals needed for MP2[16]. The criteria for calculating integrals is

$$(\mu\nu \mid \lambda\sigma)_{est} * D_{\max}(\nu,\lambda) > Threshold \tag{7}$$

Where the magnitudes of the integrals are estimated using the Cauchy-Schwarz inequality[17] and $D_{\max}$ is a test density matrix for which the (ν,λ) element is the maximum value of the product of MO coefficients for all pairs included in the transformation. Thus the scaling of the number of calculated integrals is linearized for large systems.

2.1.3.2 Neglecting the calculations of $(\mathrm{K}_{ij})^{p,q}$ with small MO coefficients

As the majority of MO coefficients for localized occupied orbitals are negligible, contributions to the internal exchange matrix's element $(\mathrm{K}_{ij})^{p,q}$ with two negligible MO coefficients can be exempted from calculation. This can be achieved by sorting MO coefficients and then using an indexing array to keep track of the original positions of the permuted MO indices.

Besides, determining local domains from purely numerical results instead of using pre-determined local domains can reduce the errors to a few micro Hartrees of canonical results[4]; a dynamic updating scheme for pair amplitudes matrices T_{ij} is used to accelerate the convergence of equation 3 and save the storage space.

2.2 Atomic orbital Laplace MP2 methods

In this method, Ayala and Scuseria used the Laplace transform method instead of an orbital invariant formulation to remove the restriction to use canonical molecular orbitals[6]. And linear scaling is realized by prescreening of AO integrals similar to 3.2.2 and by introducing the concept of atomic orbital domains such that a considerable number of pairs can be neglected thanks to the power law decay of long range correlation.

2.2.1 Laplace transform approach

The Laplace transformation was introduced to MP2 by Almlöf in 1991[18] to eliminate the energy denominators. According to Scuseria et al.[1], equation 1 can then be reformulated as

$$E_2 = -\sum_{iajb}\int_0^\infty (ia\mid jb)[2(ia\mid jb)-(ib\mid ja)]e^{-\Delta_{ijab}t}dt$$

$$= -\int_0^\infty \sum_{i'a'j'b'} (i'a'\mid j'b')[2(i'a'\mid j'b')-(i'b'\mid j'a')]dt\,, \qquad (8)$$

where $\Delta_{ijab}=\varepsilon_a+\varepsilon_b-\varepsilon_i-\varepsilon_j$, $i'=ie^{(\varepsilon_i-\varepsilon_F)t/2}$, $a'=ae^{-(\varepsilon_a-\varepsilon_F)t/2}$, ε_F is set to be the Fermi level. The above integral can be accurately carried out by Gaussian quadrature:[1,2]

$$E_2 = -\sum_{\alpha}^{\tau} w_\alpha e_2^\alpha\,, \qquad (9)$$

$$e_2^\alpha = \sum_{i^\alpha a^\alpha j^\alpha b^\alpha} (i^\alpha a^\alpha\mid j^\alpha b^\alpha)[2(i^\alpha a^\alpha\mid j^\alpha b^\alpha)-(i^\alpha b^\alpha\mid j^\alpha a^\alpha)]\,, \qquad (10)$$

$$i^{\alpha} = ie^{(\varepsilon_i - \varepsilon_F)t_\alpha/2},\ \ a^{\alpha} = ae^{-(\varepsilon_a - \varepsilon_F)t_\alpha/2}. \tag{11}$$

Micro-Hartree accuracy can be obtained with only 8-10 quadrature points. [19]

As for determining quadrature parameters $\{w_\alpha, t_\alpha\}$, one of the methods could be by least squares fit of $\frac{1}{x}$ function over the interval of values spanned by Δ_{ijab} [19].

2.2.2 AO-Laplace formulation

Here one uses the AO representation, which was formulated by Häser[20].

First they expressed expansion of the MOs in terms of contracted Cartesian Gaussian type functions:

$$|i>=\sum_{\nu}|\nu>C_{\nu i}, |a>=\sum_{\nu}|\nu>C_{\nu a}. \tag{12}$$

Here, they defined Laplace density matrices $X^{\alpha}_{\mu\nu}, Y^{\alpha}_{\mu\nu}$:

$$X^{\alpha}_{\mu\nu} = \sum_{i}^{occupied} C_{\mu i}C_{\nu i}e^{\varepsilon_i t_\alpha}, Y^{\alpha}_{\mu\nu} = \sum_{a}^{virtual} C_{\mu a}C_{\nu a}e^{-\varepsilon_a t_\alpha}. \tag{13}$$

$X^{\alpha}_{\mu\nu}, Y^{\alpha}_{\mu\nu}$ relate to occupied-occupied and virtual-virtual blocks. And to avoid the impractical eightfold summation over basis function indices when calculating e_2, they define

$$|\overline{\mu}>=\sum_{\nu}|\nu>X^{\alpha}_{\nu\mu}, |\underline{\mu}>=\sum_{\nu}|\nu>Y^{\alpha}_{\nu\mu} \tag{14}$$

Here, the ones with the overlines relate to the occupied orbitals and the ones with the underlines relate to the virtual orbitals.

Then the energy expression can be reformulated as:

$$e_2^{\alpha} = -\sum_{\mu\nu\lambda\sigma}(\underline{\mu}^{\alpha}\overline{\nu^{\alpha}}\,|\,\underline{\lambda}^{\alpha}\overline{\sigma^{\alpha}})[2(\mu\nu|\lambda\sigma)-(\mu\sigma|\lambda\nu)], \tag{15}$$

Where

$$(\underline{\mu}^{\alpha}\overline{\nu^{\alpha}}\,|\,\underline{\lambda}^{\alpha}\overline{\sigma^{\alpha}}) = \sum_{\gamma\delta\kappa\xi} X^{\alpha}_{\mu\gamma}Y^{\alpha}_{\nu\delta}(\gamma\delta|\kappa\xi)X^{\alpha}_{\kappa\lambda}Y^{\alpha}_{\xi\sigma} \tag{16}$$

2.2.3 Prescreening of AO integrals

To reduce the computational cost, the first step is to screen the negligible AO integrals by introducing four two-index matrices, which is in the spirit of the Schwarz based screening, similar to 3.1.3. And for convenience, α is omitted from formula. The two-index matrices A, B, C, D are defined as following,

$$A_{\mu\nu} = |(\mu\nu|\mu\nu)|^{\frac{1}{2}}, B_{\mu\nu} = |(\underline{\mu}\nu|\underline{\mu}\nu)|^{\frac{1}{2}}, C_{\mu\nu} = |(\mu\overline{\nu}|\mu\overline{\nu})|^{\frac{1}{2}}, D_{\mu\nu} = |(\underline{\mu}\overline{\nu}|\underline{\mu}\overline{\nu})|^{\frac{1}{2}} \tag{17}$$

Taking advantage of the Schwarz inequality, one can partially screen out partially transformed integrals depending on their contribution to e_2. Take the quarter transformed

integrals $(\mu\bar{\nu}\,|\,\lambda\sigma)$ for example, they will only be calculated if $C_{\nu\mu}A_{\lambda\sigma}[2\mathrm{B}_{\mu\nu}\mathrm{D}_{\lambda\sigma}+\mathrm{B}_{\sigma\nu}\mathrm{D}_{\lambda\mu}]$ is larger than a chosen threshold θ. Then based on this screening scheme, all four quarter transformations of AO integrals are performed.

Now let us evaluate the above AO-Laplace MP2 method in terms of computational cost. For the transformation part, although the transformation in the AO basis is supposed to be more computationally expensive than in the MO basis, this screening scheme makes these two comparable. Also it is demonstrated that the whole algorithm is only quadratic scaling[6].

2.2.4 Atomic orbital domains

It has been demonstrated that the interaction that survive in O(N^2) asymptote is the long range correlation which decays with the power law of the distance between two molecular segments[6]. So to reach linear scaling, selective interactions between two segments should be neglected.

In the spirit of this, Scuseria et al.[6] defined atomic orbital domains as following: for each atomic orbital μ, there is an interaction domain which is a sphere centered on μ, and charge distribution $\gamma\delta$ will be considered to belong to domain D(μ) if $(X_{\mu\gamma}S_{\gamma\delta}Y_{\delta\mu})^2$ exceeds a threshold ε, where S is the overlap matrix.

The radius of the sphere is defined by the maximum distance between μ and $\gamma\delta$. And the long-range contribution of the μ and λ pair, $(\underline{\mu}\bar{\mu}|\underline{\lambda}\bar{\lambda})$ $(\mu\mu|\lambda\lambda)$, will be neglected if the edges of the domains are separated more than WS Bohrs from each other. In this way, linear scaling is reached.

A systematic way was designed to determine ε and WS such that a certain accuracy could be reached by making ε small enough and WS large enough. Scuseria et al.[6] demonstrated that given the selection threshold for the AO domains ε and the threshold used in Schwarz screening θ, WS can be determined. In this way, the errors are well defined in this algorithm.

Thus a remarkable advantage of this method is that it can reproduce MP2 energies which is obtained by conventional methods, while keeping linear scaling computational cost.

2.3 Density fitting LMP2

The above methods have two common problems. Firstly, to reach linear scaling, the system should be rather extended, such as one dimensional alkanes or peptide chains, whereas for the compact three-dimensional systems, the linear scaling is not as good. Secondly, large basis sets are needed to obtain a certain accuracy. However, the fourth order dependence on the basis set size limits the use of large basis sets.

To solve the above problems, density fitting (DF) methods[8,21-27] are introduced, which is originally called resolution of identity. As the origin of the fourth order dependence on the basis set size for LMP2 methods is the calculation of the 4-index 2-electron integrals (i,a|j,b) and the transformation from the AO to local orbital basis, in DF-MP2 methods the one-electron charge densities are approximated by linear expansions in an auxiliary basis set. In this way, 4-index 2-electron integrals can be written in terms of two 3-index 2-electron integrals.

DF methods can lead to two kinds of savings: the dependence of computational cost on the basis set size is third order instead of fourth order; the 3-index integrals are much faster to transform than 4-index integrals. While the prefactor of scaling is much smaller than conventional MP2, the scaling of the cost with the molecular size, however, is still $O(N^5)$. Werner et al.[8] combined the DF-MP2 and the local correlated methods, which leads to DF-LMP2. In this method, they use the approximation similar to the method of Pulay, that is, the use of local domains for each electron pair and the use of multiple expansions for distant pairs. This would lead to $O(N^2)$ scaling. Then Werner et al. further reduce the scaling to O(N) by using different fitting bases for each electron pair.

In Section 3.3.1, more theoretical details of the DF-MP2 will be introduced; in Section 3.3.2, DF-MP2 methods will be combined with a local correlated method.

2.3.1 Conventional DF-MP2

The DF-MP2 was first introduced by Feyreissen et al.[21,27]. By adding the identity matrix $I = \sum_A |A><A|$, the 4-index two-electron integrals $K_{ab}^{ij} = (i,a \mid j,b)$ can be rewritten as[4]:

$$K_{ab}^{ij} = \sum_A (i,a \mid A)(A \mid j,b) \tag{18}$$

Where |A> is an orthonormal fitting basis function, which in the wavefunction expression is $\chi_A(r)$, and the summation is over the complete fitting basis.

To generalize Equation 18, different fitting functions should be used. It was demonstrated[8] that Equation 18 can be written as:

$$K_{ab}^{ij} = \sum_{AB} (i,a \mid A)[J^{-1}]_{AB}(B \mid j,b) \tag{19}$$

where

$$J_{AB} = \int dr_1 \int dr_2 \frac{\chi_A(r_1)\chi_B(r_2)}{r_{12}} \tag{20}$$

$$(i,a \mid A) = \int dr_1 \int dr_2 \frac{i(r_1)a(r_1)\chi_A(r_2)}{r_{12}} \tag{21}$$

(i,a|A) is a three-index two-electron integral, which needs a two-step transformation from three-index integrals $(\mu,\nu \mid A)$ in the AO basis.

Equation 19 is exact if the fitting basis sets are complete. However, in reality, they are incomplete, and this will lead to an error. Fortunately, it has been shown that with suitable fitting basis sets, the errors are much smaller than other typical errors in the calculation.[28]

2.3.2 Local Density Fitting MP2 (DF-LMP2)

Similar to Pulay's methods, the occupied space is spanned by localized molecular orbitals, and the virtual space is spanned by a basis of nonorthogonal projected atomic orbitals (PAOs).

Using these localized orbitals, two approximations will dramatically reduce the calculation cost. First, each occupied orbital i is assigned with a subset of PAO, i.e. truncated virtual domain D(i), similar to Section 3.1.2. As the virtual domain size is independent of the molecular size, a lot of computational cost is saved. Second, integrals for distant pairs can be approximated by multipole expansions, or neglected. Thus the remaining number of pairs increases linearly with molecular size. It has been proved[8] that utilizing these two approximations, the scaling will be $O(N^2)$.

To further decrease the scaling, there are two strategies[8]. In the first strategy, different fitting basis sets are used for different electron pairs. The concept of domains also applies to the fitting basis. That is to say, the fitting basis for a given pair (i, j) comprises the union of the truncated virtual domain D(i) and D(j), denoted as $[ij]_{fit}$. Thus, the size of the fitting basis sets is independent of the molecular size. Another strategy is that fitting is performed only once for each orbital i, i.e. orbital fit domain $[i]_{fit}$ is assigned for each orbital i. However, the number of fitting functions in the orbital fit domains is larger than in the first strategy.

Similar to Section 3.1.3.1, to linearize the integral evaluation, the Schwarz inequality is used to estimate the 3-index integral $(\mu, \nu \mid A)$ to screen some negligible integrals.

$$(\mu, \nu \mid A) \leq (\mu, \nu \mid \mu, \nu)^{\frac{1}{2}} (A \mid A)^{\frac{1}{2}} \tag{22}$$

Depending on this value of this product, one can figure out which orbital i will contribute to the transformation. For the survived orbital i, a lookup table is established to test whether a certain A is needed or not. If not, the integral and the transformation can be omitted from the calculation.

2.4 Discussion

Although these three methods use different strategies to linearize the calculation, they have something in common. The essence of these methods is the same, i.e., localizing the orbitals in order to reduce the number of the integrals to be calculated. For example, they all use a screening procedure to screen out the insignificant integrals, and orbital domains are all introduced in these three methods.

However, each method has different features. The Pulay's method is the first LMP2 method and all other LMP2 methods originate from it. Also a lot of improvements have been made towards increasing the accuracy and efficiency of this method. So this method is quite mature. AO-LMP2 method has strict proof towards linearity of the calculation of the methods and they invented a systematic way to improve the accuracy[6], which would facilitate the further development of their method. And the crucial improvement made by density fitting method is that four-index two-electron integrals are approximated by the two three-index integrals, while the other parts of the method are in essence the same with Pulay's method. And as a result, DF-LMP2 method leads to a smaller pre-factor and less dependence on the basis set size. All these three methods have reported that essentially identical results (within micro-Hartree accuracy) with the conventional MP2 methods have been achieved.[4,6,8]

As for the comparison between these methods, it is difficult to compare since test calculations have been performed on different computers and on (at least slightly) different molecular systems.

3. Applications

3.1 DNA systems

In this section, the LMP2 methods will be applied to DNA systems with more than 500 atoms and more than 5000 basis functions [29] and it is demonstrated that the low scaling has been reached.

3.1.1 Methods

AO Laplace MP2 methods are the main methods here. To reduce the dependency on the basis set size of AO-MP2, a Cholesky decomposition of the Laplace density matrices $X_{\mu\nu}^{\alpha}, Y_{\mu\nu}^{\alpha}$ (CDD) was used. With Cholesky decomposition, the Laplace density matrices can be written as:

$$X_{\mu\nu}^{\alpha} = \underline{L}\underline{L}^{T}, Y_{\mu\nu}^{\alpha} = \overline{L}\overline{L}^{T} \tag{23}$$

Where $\underline{L}$ and $\overline{L}$ are lower triangle matrixes and can be considered as the coefficients of localized occupied (virtual) pseudo-MOs (LPMOs). This is the so-called CDD-MP2 method, which was first introduced in 2009.[30] In this way, the CDD-MP2 energy can be written as:

$$E_{CDD-MP2} = -\sum_{\alpha}\sum_{ij}^{occ}\sum_{ab}^{virt}[2(\underline{i}\overline{a}\,|\,\underline{j}\overline{b}) - (\underline{i}\overline{b}\,|\,\underline{j}\overline{a})](\underline{i}\overline{a}\,|\,\underline{j}\overline{b}) \tag{24}$$

where the two-electron integrals in the basis of LPMOs,

$$(\underline{i}\overline{a}\,|\,\underline{j}\overline{b}) = \sum_{\mu\nu\lambda\sigma}\underline{L}_{\mu i}\overline{L}_{\nu a}\underline{L}_{\lambda j}\overline{L}_{\sigma b}(\mu\nu\,|\,\lambda\sigma)\,. \tag{25}$$

In addition, an efficient QQR-type estimate, which depends on the charge distribution and charge distance, for significant integral products was used in the implementation of the AO-MP2 method. The QQR-type integral estimates take the form

$$(\underline{i}\overline{a}\,|\,\underline{j}\overline{b}) \le \frac{Z_{\underline{i},\max} Z_{\underline{j},\max}}{(R_{\underline{i},\underline{j}} - ext_{\underline{i}} - ext_{\underline{j}})^{3}} \tag{26}$$

Where $Z_{\underline{i},\max} = \max_{\overline{a}} Z_{\underline{i},\overline{a}} = (\underline{i}\overline{a}\,|\,\underline{i}\overline{a})^{\frac{1}{2}}$, $R_{\underline{i},\underline{j}}$ is the distance between the centers of two LPMOs and $ext_{\underline{i}}$ is the extent of the occupied LPMO $\underline{i}$. Detailed definition of the above parameters can be found in the appendix C of ref[29]

As for the calculation of electron repulsion integrals in the LPMO basis, the density fitting approximation was used.

To summarize, the use of Cholesky decomposed Laplace density matrices is used within the framework of Laplace-transform MP2 theory, leading to the so-called CDD-MP2 method. And QQR-type estimates are used for the prescreening of negligible integrals, while density fitting methods are used to evaluate the electron repulsion integrals.

3.1.2 Results on DNA systems

Calculations on very large DNA systems are made in a def2-SVP basis.[29] The calculated system contains 16 base pairs and 1052 atoms, and the def2-SVP basis has 11230 basis functions. And the calculation was performed in parallel on two Xeon E5645 processors with 12 cores. The RI-CDD-MP2 calculation time was ~49.5 days[29], while for a conventional RI-MP2 calculation, an optimistic extrapolation would lead to two years of CPU time and another year for serial I/O operations.

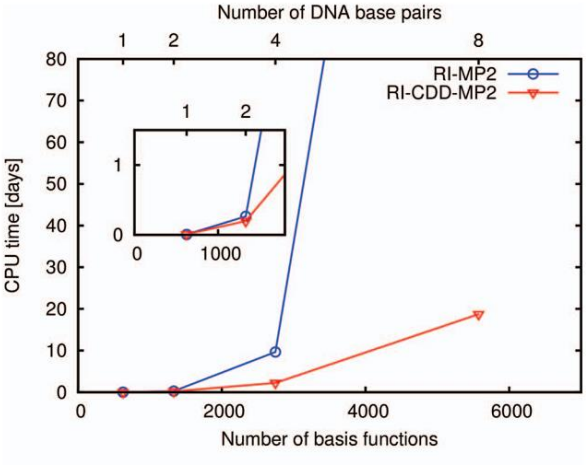

Fig.1[29] Timings of their RI-CDD-MP2 method in comparison to canonical RI-MP2 on DNA systems. The RI-MP2 values for the largest DNA systems (8 base pairs in def2-SVP) have been conservatively extrapolated with the scaling behavior of the two previous points.

3.2 CRYSCOR: a program for 1D-, 2D- and 3D-periodic systems

Based on the efficient and parallel implementation of density fitted periodic LMP2, a program called CRYSCOR[31,32], which can be used to study 1D-, 2D- and 3D- periodic systems, was launched by C. Pisani et al. in 2000. The program can be used to calculate the following parameters: 1. correlation energy; 2. MP2 one-electron position density matrix; 3. The MP2 one-electron momentum density matrix; 4. excitonic band gaps. In addition, according to 2 and 3, electron charge density and Compton profiles can be deduced, which reflects the chemical composition, geometry and momentum space of the system. Here, we will discuss the following applications[32]: (a) calculation of rolling energy of a one-dimensionally periodic boron nitride (BN) nanoscroll; (b) absorption of argon on the MgO (100) surface; (c) relative energy of 3D covalent crystals: aluminosilicate polymorphs.

3.2.1 Rolling energy of a one-dimensionally periodic boron nitride (BN) nanoscroll

A nanoscroll is a spirally wrapped stripe with a 1D tubular structure resembling that of a multiwalled carbon nanotube (cf. Fig 2[32]). Here, rolling energy, which is the energy difference between a BN nanoscroll and the related nanostripe, is calculated.

The system of interest has a honeycomb arrangement of B and N atoms and two borders saturated with hydrogen atoms. Thus in each unit cell, there are 60 B, 60N and 2 H atoms, and the rolling energy per BN unit can be written as:

$$E^{roll} = (E^{scroll} - E^{stripe}) / 60 \tag{27}$$

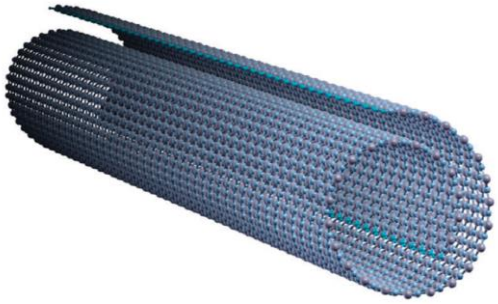

Fig.2[32] A portion (45 unit cells are pictured) of the one-dimensionally periodic rolled nano-scroll

Results of three different methods are listed in table 1. We can see that DFT methods using B3LYP functional and HF methods revealed that the rolled configuration is not preferable, which does not agree with the experimental results. And only MP2 correlation correction is capable of predicting the right stability.

Table 1 comparison of the rolling energy obtained by different methods

	DFT (B3LYP) kcal/mol	HF kcal/mol	HF+Density fitting LMP2 kcal/mol
E^{roll}	16.05	5.72	-4.6

3.2.2 Absorption of argon on the MgO (100) surface

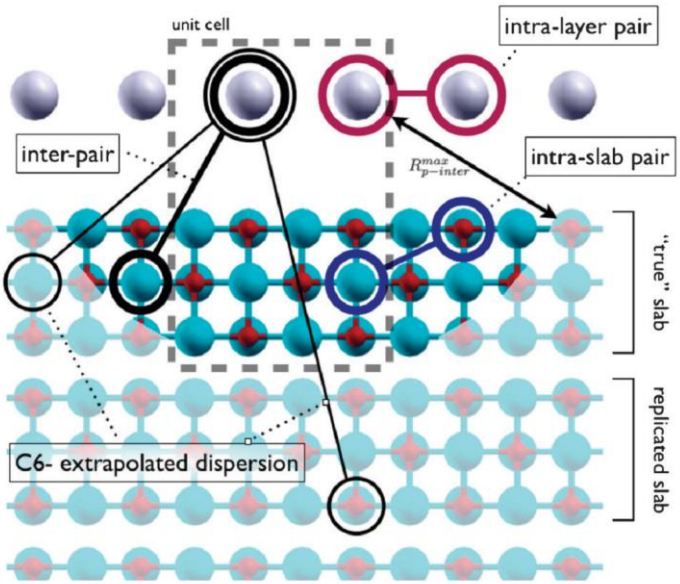

Fig.3[32] Schematic representation of the correlation energy partitioning in the local MP2 method and the model of the semi-infinite crystal for the dispersion interaction

The case of the 2×2 square argon monolayer adsorption on the MgO (100) surface) is

considered here. There are three different adsorbing sites of MgO (100), i.e., on oxygen, on magnesium, and on the midpoint between two adjacent Mg atoms, respectively. The adsorption energy consists of the HF adsorption energy and the correlation part, which is partitioned into intra-slab, intra-adsorbate, and inter-slab-adsorbate components (cf. Fig.3[32]).

The calculation results are shown in Fig. 4[32]. The three curves of different colors represent interacting energy and its components on different adsorbing sites. First, let us look at long range. The three potential curves (related to three different adsorption sites) coincide at long range, which is a result of isotropy of dispersive interactions.

Next, at short range, the dominating component is the exponentially growing exchange repulsion, and the three different potential curves start to differentiate from each other. The reason for the difference can be understood according to the difference electron density of different adsorption sites. For example, for the on-O position, the repulsive onset starts at larger distance, which is due to the fact that in the MgO slab the electron density is concentrated around the oxygen atoms.

If we combine the effect of both the long range dispersion and short range repulsion, we can conclude that the most preferable adsorption site is the on-Mg position.

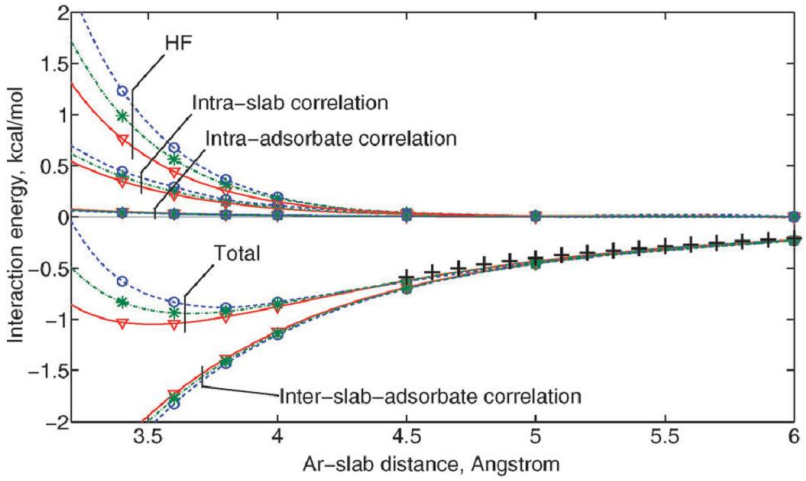

Fig. 4[32] The interaction energy and its components (HF, intra-slab, inter-slab-adsorbate and intra-adsorbate) between a three-layer MgO (001)-slab and the argon monolayer in the 2 × 2 supercell arrangement (one argon atom per two Mg atoms on the surface). The on-O (blue/ spheres/ dashed), on-Mg (red/triangles/solid), and Mg–Mg bridging (green/stars/dash-dotted) adsorption positions are considered.

3.2.3 Relative energy of 3D covalent crystals: aluminosilicate polymorphs

The relative stability of Al_2SiO_5 ortho-silicate polymorphs (Kyanite, K, Andalusite, A, and Sillimanite, S, whose structures are shown in Fig.5[32]) is of great interest in the context of simulation of geological processes. However, from the experimental aspect, the error bars exceed the energy differences between three polymorphs, while the DFT methods exhibit a larger variation of values depending on the choice of the exchange-correlation functional. Thus the relative stability is calculated by LMP2 methods.

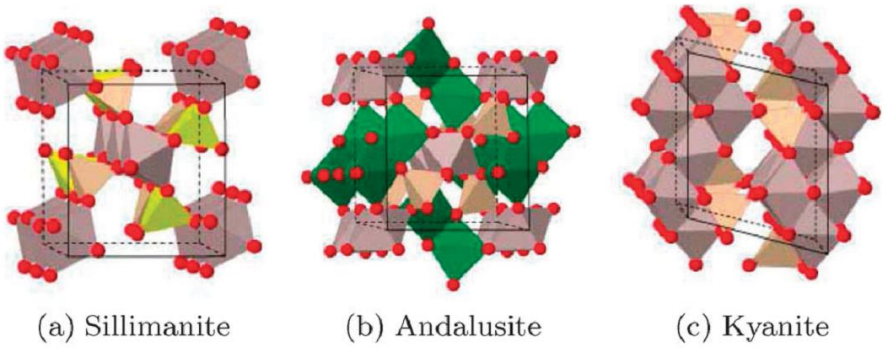

Fig.5[33] Crystalline structure of three Al_2SiO_5 polymorphs. Hexa-, penta-, and tetra-coordinated aluminium atoms are represented in gray, green and yellow, respectively; silicon and oxygen tetrahedra are in beige and red, respectively.

To calculate the stability, all contributions to the Gibbs free energy should be considered, i.e., the electronic, the pressure-volume, the entropic, and the zero point terms. However, only the electronic contribution contributes most to the relative stability[33], and thus only the electronic contribution is calculated here.

The results obtained by the HF method, HF+LMP2 method as well as the DFT (using different functionals) methods are shown in table 2. Experimental results are taken from ref[34] and ref[35]. We can see from the table that the DFT results vary a lot according to the different functionals; the HF method does not succeed in predicting the trend; and the relative stability calculated by HF+LMP2 method is K>S>A, which agrees with the experiments quite well, except that a certain overestimation of the A-K stability. This may be due to the neglect of other contributions to the Gibbs free energy.

Table 2 Relative energy (in kJ mol^{-1} per Al_2O_3 unit) of A and S with respect to K. The geometries used in the MP2 calculations were optimized at the PBE0 level

	A-K	S-K
HF	-19.17	-22.61
SVWN(LDA)	22.26	36.88
PW91(GGA)	-5.21	4.88
PBESOL(GGA)	10.32	26.36
B3LYP(hybrid)	-16.50	-13.90
PBE0(hybrid)	-0.34	10.93
PBE0-D2(hybrid+disp)	35.76	33.66
HF+MP2	17.66	4.94
Exp[35]	-16.50	-13.90
Exp[34]	3.86	7.72

3.3 Cohesive Energy of Molecular Crystals

In this application, Usvyat et al. used LMP2 to calculate the cohesive energy of the molecular crystal: CO_2.[36] The cohesive energy is the energy required to break all the bonds associated with

one of its constituent molecules. It is therefore a measure of the inter-molecular energy for a substance. However, for molecular crystals, as the long range correlation (dispersion) is the main binding contribution, an accurate description of long range correlation is needed. DFT methods can in general not be used in calculating dispersion, while post-HF methods are quite expensive. Thus, local MP2 methods are used here, and to guarantee certain accuracy, it is combined with an incremental correlated calculation. In the following discussion, the method of increments is first discussed, and then the LMP2 and method of increments are combined and applied to the CO_2 molecular crystal.

3.3.1 Method of Increments

This method was first introduced by H. Stoll and co-workers to calculate the correlation energy of a solid.[37-39]

The idea of the incremental methods is based on a many body expansion of the energy of a solid,

$$E^{incr} = \sum_{L} \varepsilon_L + \sum_{LM} \Delta\varepsilon_{LM} + \sum_{LMN} \Delta\varepsilon_{LMN} + \ldots \tag{28}$$

where L, M, N… represent the valence orbitals at one molecule, i.e. one center; ε_L, the one center terms, are the energies of single molecules; $\Delta\varepsilon_{LM}$, $\Delta\varepsilon_{LMN}$, etc., the "many center" terms, are the two-body, three-body, etc. interactions between molecules:

$$\Delta\varepsilon_{LM} = \varepsilon_{LM} - (\varepsilon_L + \varepsilon_M) \tag{29}$$

$$\Delta\varepsilon_{LMN} = \varepsilon_{LMN} - (\Delta\varepsilon_{LM} + \Delta\varepsilon_{LN} + \Delta\varepsilon_{MN} + \varepsilon_L + \varepsilon_M + \varepsilon_N) \tag{30}$$

…

The first sum over L in Equation 28 runs over all molecules in one unit cell, while the range for the other sums is not restricted. In practice, a cutoff radius is used to restrict these sums, similar to the truncation of the virtual space in LMP2.

Thus the incremental expansion of the cohesive energy of a molecular crystal is

$$\Delta E = E^{incr} - \sum_{L} E_L^{mol} . \tag{31}$$

Or if we write

$$\Delta\varepsilon_L = \varepsilon_L - E_L^{mol} , \tag{32}$$

which has the meaning of the one-body term of the cohesive energy incremental series, thus the cohesive energy can be rewritten as

$$\Delta E = \sum_{L} \Delta\varepsilon_L + \sum_{LM} \Delta\varepsilon_{LM} + \sum_{LMN} \Delta\varepsilon_{LMN} + \ldots \tag{33}$$

The general procedure for the standard incremental methods is the following:[37] (a) Starting from output data of a standard SCF calculation, localized atom-centered and/or bond orbitals are generated according to a suitable localization procedure. (b) "One-body" correlation energy increments, $\Delta\varepsilon_L$, are then generated by correlating each of the localized orbitals in turn, while

keeping the other ones inactive. (c) "Two-body" increments, $\Delta\varepsilon_{LM}$, are next determined by considering pairs of localized orbitals, and performing correlated calculations for each chosen pair, allowing excitations from this pair only and keeping the rest of the orbitals inactive as before. (d) Higher-order increments are defined in an analogous way. (e) Adding all of these increments, with the proper weight factors (according to their occurrence in the solid), one obtains an estimate of the correlation energy of the crystal.

One of the bottlenecks for the incremental method is the slow convergence due to the long-range and many body electrostatic and induction contributions. A way to improve this is to use a periodic HF[40], LCCSD or DFT[41] treatment, or to introduce embedding cluster, as they can incorporate the influence of the low-order long-range and many-body effects on the correlation energy.

3.3.2 Incrementally Corrected Periodic LMP2 Scheme

The Pulay's LMP2 scheme is used here, i.e. two types of local approximations are made here: the first is the domain approximation, where the virtual space is truncated to a certain domain (refer to 3.1.2); the second is truncating the list of correlated electron pairs according to the distance between the pairs.

Using the periodic LMP2 methods, the main fraction of the cohesive energy for molecular crystals is obtained. Then in the same spirit of the progressive down-sampling technique, the incremental methods are only used for corrections rather than the whole correlation energy and thus faster convergence of the incremental expansion can be guaranteed.

There are two kinds of corrections that incremental methods can be applied to. One is the basis set correction, δE_{BSC} , which is defined as the difference between the basis set extrapolated energy and the energy obtained with the basis set of the periodic calculations [in this case (A)VTZ],

$$\delta E_{BSC} = \Delta E^{incr}_{LMP2/BSL} - \Delta E^{incr}_{LMP2/(\mathrm{A})\mathrm{VTZ}} \tag{34}$$

Another correction is the post-MP2 energy contribution, $\delta E_{post-MP2}$, which is defined as the incrementally calculated difference between the CCSD(T) and MP2 [or LCCSD(T0) (here, T0 means local triplet) and LMP2] energies

$$\delta E_{post-MP2} = \Delta E^{incr}_{CCSD(T)} - \Delta E^{incr}_{MP2} \tag{35}$$

3.3.3 Results

The following calculations were carried out using the CRYSTAL [42] (periodic HF), CRYSCOR [32] (periodic LMP2), and MOLPRO[43] (incremental calculations) packages.

Different schemes are used to calculate the cohesive energy of CO_2 to compare the efficiency and accuracy. One scheme is to calculate the cohesive energy directly by incremental LMP2, incremental LMP3, or incremental LCCSD(T0) methods; another scheme is first to perform

a LMP2 calculation and use the incremental methods to correct this calculation (results of this scheme are shown in the bold font in table 3).

Table 3. Cohesive Energy Contributions for CO_2 from Increments Calculated with Embedded Clusters[36]

	one-body (kJ/mol)	two-body (kJ/mol)	three-body (kJ/mol)	Total (kJ/mol)
LMP2	+12.04	-38.54	+0.04	-26.47
LMP3	+7.93	-29.76	+2.08	-19.74
LMP3-LMP2	**-4.11**	**+8.78**	**+2.04**	**+6.71**
LCCSD(T0)	+10.20	-37.54	+0.71	-26.63
LCCSD(T0)-LMP2	**-1.84**	**+1.00**	**+0.67**	**-0.16**

**Bold font indicates post-MP2 energy corrections*

We can see from the table that when using the post MP2 corrections, the deviations of the incremental correlation energies virtually disappear (+6.71kJ/mol for LMP3-LMP2 and -0.16kJ/mol for LCCSD(T0)-LMP2). We can conclude that a combination of the incremental methods and LMP2 methods is more accurate than the standard incremental method.

Now let us compare the convergence. First look at Fig. 1. The curves of hollow diamonds and hollow squares are obtained by standard incremental methods and the incremental expansion of complete correlation energy is used, while those of solid diamonds and squares are obtained using incremental expansion of $\delta E_{post-MP2}$. We can draw from Fig. 6 the conclusion that the incremental expansion of $\delta E_{post-MP2}$ converges with the cutoff interatomic distance of the clusters included in the calculations much faster than that for the complete correlation energy. This means that in standard incremental calculations, a large number of clusters are needed to be included, which will make this method relatively expensive.

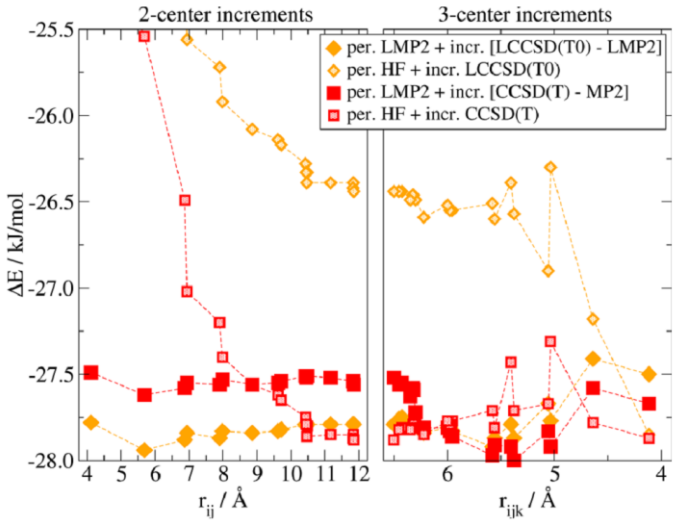

Fig. 6[36] Convergence of two- and three-center incremental CCSD(T) and LCCSD(T0) cohesive energies for CO_2 added to the periodic HF result, and CCSD(T)−MP2 and LCCSD(T0)−LMP2 corrections added to the periodic HF + LMP2 result, as functions of the maximal averaged distance between atoms belonging to different molecular units in bare $(CO_2)_2$ or $(CO_2)_3$ clusters.

Next, let us look at Fig. 7. It shows the cohesive energy calculated (i) with the incremental MP2 and LMP2 energies extrapolated to the basis set limit and (ii) with the periodic LMP2 energies plus the incremental basis set correction, both as functions of the inter-center cutoff for the two-body clusters. As discussed above, the one calculated with complete correlation energy converges relatively slow, but the incremental basis set correction δE_{BSC}, similar to the method error correction $\delta E_{post-MP2}$, exhibits extremely rapid convergence.

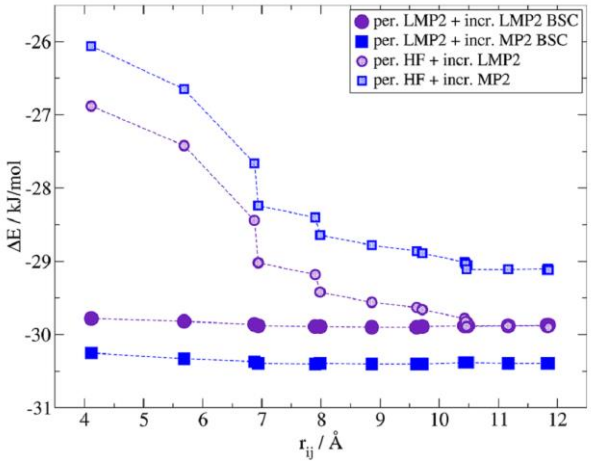

Fig. 7[36] Convergence of the two-center incremental MP2 and LMP2 cohesive energies for CO_2 extrapolated to the basis set limit and added to the periodic HF result, along with the basis set corrections added to the periodic HF + LMP2 result as functions of the maximal averaged distance between atoms belonging to different molecular units in bare $(CO_2)_2$ clusters.

4. Discussion and suggestions for future work

Although LMP2 methods have witnessed a tremendous development during these years, they still have quite a few problems. One is that the efficiency is still not good enough to calculate the interesting systems. For example, one chromosome of a human contains thousands of atoms, which will lead to trouble if calculated by the existing methods. The efficiency can be improved by considering the following aspects. Firstly, we can improve parallelization of LMP2 method. Nowadays, parallelization of LMP2 has been implemented on a small scale, and a larger scale is needed. Second, new strategies should be introduced to improve the localizability of the orbitals, which will decrease the number of the pairs that is needed to be calculated.

Another problem is the accuracy problem. For this problem, we can resort to the LCCSD method. A combination of these two methods may be useful to guarantee both the accuracy and efficiency. Also, a powerful and accurate estimation of integrals should be introduced to make a better screening of the negligible integrals and less unwanted screening of the large integral contributions.

Last but not least, a unified standard should be established to compare the results for different methods. Although at the moment, benchmark calculations are implemented by most of the methods, it is still difficult to compare the efficiency and the accuracy as there is no clear unified standard for all the theoretical chemists to follow. As a result, it is really difficult to make a judgement of different methods.

Hopefully, despite the existing problems, with the development of the local correlated methods, computational chemistry will make a crucial contribution to the insight into the interesting nanosystems.

5. Reference

1 Saebo, S. & Pulay, P. The local correlation treatment. II. Implementation and tests. *The Journal of Chemical Physics* **88**, 1884-1890 (1988).

2 Pulay, P. Localizability of dynamic electron correlation. *Chemical Physics Letters* **100**, 151-154, doi:http://dx.doi.org/10.1016/0009-2614(83)80703-9 (1983).

3 Sæbø, S. & Pulay, P. Local configuration interaction: An efficient approach for larger molecules. *Chemical Physics Letters* **113**, 13-18, doi:http://dx.doi.org/10.1016/0009-2614(85)85003-X (1985).

4 Saebø, S. & Pulay, P. A low-scaling method for second order Møller–Plesset calculations. *The Journal of Chemical Physics* **115**, 3975-3983, doi:doi:http://dx.doi.org/10.1063/1.1389291 (2001).

5 Schütz, M., Hetzer, P. & Werner, H.-J. Low-order scaling local electron correlation methods. I. Linear scaling local MP2. *The Journal of Chemical Physics* **111**, 5691, doi:10.1063/1.479957 (1999).

6 Ayala, P. Y. & Scuseria, G. E. Linear scaling second-order Moller–Plesset theory in the atomic orbital basis for large molecular systems. *The Journal of Chemical Physics* **110**, 3660-3671, doi:doi:http://dx.doi.org/10.1063/1.478256 (1999).

7 Murphy, R. B., Beachy, M. D., Friesner, R. A. & Ringnalda, M. N. Pseudospectral localized MØller-Plesset methods: Theory and calculation of conformational energies. *The Journal of Chemical Physics* **103**, 1481-1490, doi:10.1063/1.469769 (1995).

8 Werner, H.-J., Manby, F. R. & Knowles, P. J. Fast linear scaling second-order Møller-Plesset perturbation theory (MP2) using local and density fitting approximations. *The Journal of Chemical Physics* **118**, 8149-8160, doi:doi:http://dx.doi.org/10.1063/1.1564816 (2003).

9 Boys, S. Localized orbitals and localized adjustment functions. *Quantum Theory of Atoms, Molecules, and the Solid State, A Tribute to John C. Slater* **1**, 253 (1966).

10 Pulay, P., Saebo/, S. & Meyer, W. An efficient reformulation of the closed‐shell self‐consistent electron pair theory. *The Journal of Chemical Physics* **81**, 1901-1905, doi:doi:http://dx.doi.org/10.1063/1.447863 (1984).

11 Pulay, P. & Saebø, S. Orbital-invariant formulation and second-order gradient evaluation in Møller-Plesset perturbation theory. *Theoret. Chim. Acta* **69**, 357-368, doi:10.1007/BF00526697 (1986).

12 Saebo, S. & Pulay, P. Fourth‐order Mo/ller–Plessett perturbation theory in the local correlation treatment. I. Method. *The Journal of Chemical Physics* **86**, 914-922, doi:doi:http://dx.doi.org/10.1063/1.452293 (1987).

13 Hetzer, G., Pulay, P. & Werner, H.-J. Multipole approximation of distant pair energies in local MP2 calculations. *Chemical Physics Letters* **290**, 143-149, doi:http://dx.doi.org/10.1016/S0009-2614(98)00491-6 (1998).

14 Schaefer III, H. F. Methods of electronic structure theory. (1977).

15 Saebo, S. & Pulay, P. Local treatment of electron correlation. *Annual Review of Physical Chemistry* **44**, 213-236 (1993).

16 Rauhut, G., Pulay, P. & Werner, H.-J. Integral transformation with low-order scaling for large

local second-order Møller–Plesset calculations. *Journal of Computational Chemistry* **19**, 1241-1254, doi:10.1002/(SICI)1096-987X(199808)19:11<1241::AID-JCC4>3.0.CO;2-K (1998).

17 Helgaker, T., Jørgensen, P. & Olsen, J. (Wiley, Chichester ;, 2000).

18 Almlöf, J. Elimination of energy denominators in Møller—Plesset perturbation theory by a Laplace transform approach. *Chemical Physics Letters* **181**, 319-320, doi:http://dx.doi.org/10.1016/0009-2614(91)80078-C (1991).

19 Häser, M. & Almlöf, J. Laplace transform techniques in Mo/ller–Plesset perturbation theory. *The Journal of Chemical Physics* **96**, 489-494, doi:doi:http://dx.doi.org/10.1063/1.462485 (1992).

20 Häser, M. Møller-Plesset (MP2) perturbation theory for large molecules. *Theoret. Chim. Acta* **87**, 147-173, doi:10.1007/BF01113535 (1993).

21 Vahtras, O., Almlöf, J. & Feyereisen, M. W. Integral approximations for LCAO-SCF calculations. *Chemical Physics Letters* **213**, 514-518, doi:http://dx.doi.org/10.1016/0009-2614(93)89151-7 (1993).

22 Weigend, F. & Häser, M. RI-MP2: first derivatives and global consistency. *Theor Chem Acta* **97**, 331-340, doi:10.1007/s002140050269 (1997).

23 Bernholdt, D. E. & Harrison, R. J. Fitting basis sets for the RI-MP2 approximate second-order many-body perturbation theory method. *The Journal of Chemical Physics* **109**, 1593-1600, doi:doi:http://dx.doi.org/10.1063/1.476732 (1998).

24 Weigend, F., Häser, M., Patzelt, H. & Ahlrichs, R. RI-MP2: optimized auxiliary basis sets and demonstration of efficiency. *Chemical Physics Letters* **294**, 143-152, doi:http://dx.doi.org/10.1016/S0009-2614(98)00862-8 (1998).

25 Hattig, C. Optimization of auxiliary basis sets for RI-MP2 and RI-CC2 calculations: Core-valence and quintuple-[small zeta] basis sets for H to Ar and QZVPP basis sets for Li to Kr. *Phys Chem Chem Phys* **7**, 59-66, doi:10.1039/B415208E (2005).

26 Hellweg, A., Hättig, C., Höfener, S. & Klopper, W. Optimized accurate auxiliary basis sets for RI-MP2 and RI-CC2 calculations for the atoms Rb to Rn. *Theor Chem Acta* **117**, 587-597, doi:10.1007/s00214-007-0250-5 (2007).

27 Feyereisen, M., Fitzgerald, G. & Komornicki, A. Use of approximate integrals in ab initio theory. An application in MP2 energy calculations. *Chemical Physics Letters* **208**, 359-363, doi:http://dx.doi.org/10.1016/0009-2614(93)87156-W (1993).

28 Weigend, F., Köhn, A. & Hättig, C. Efficient use of the correlation consistent basis sets in resolution of the identity MP2 calculations. *The Journal of Chemical Physics* **116**, 3175-3183, doi:doi:http://dx.doi.org/10.1063/1.1445115 (2002).

29 Maurer, S. A., Clin, L. & Ochsenfeld, C. Cholesky-decomposed density MP2 with density fitting: Accurate MP2 and double-hybrid DFT energies for large systems. *J Chem Phys* **140** (2014).

30 Zienau, J., Clin, L., Doser, B. & Ochsenfeld, C. Cholesky-decomposed densities in Laplace-based second-order Møller–Plesset perturbation theory. *The Journal of Chemical Physics* **130**, 204112, doi:doi:http://dx.doi.org/10.1063/1.3142592 (2009).

31 Hammerschmidt, L., Maschio, L., Muller, C. & Paulus, B. Electron Correlation at the MgF2(110) Surface: A Comparison of Incremental and Local Correlation Methods. *J Chem Theory Comput* **11**, 252-259, doi:Doi 10.1021/Ct500841b (2015).

32 Pisani, C. *et al.* CRYSCOR: a program for the post-Hartree-Fock treatment of periodic systems. *Phys Chem Chem Phys* **14**, 7615-7628 (2012).

33 Demichelis, R., Civalleri, B., Ferrabone, M. & Dovesi, R. On the performance of eleven DFT functionals in the description of the vibrational properties of aluminosilicates. *International Journal of Quantum Chemistry* **110**, 406-415, doi:10.1002/qua.22301 (2010).

34 Olbricht, W., Chatterjee, N. & Miller, K. Bayes estimation: A novel approach to derivation of internally consistent thermodynamic data for minerals, their uncertainties, and correlations. Part I: Theory. *Phys Chem Minerals* **21**, 36-49, doi:10.1007/BF00205214 (1994).

35 Bergaya, G. L. F. & Theng, B. K. G. *Handbook of Clay Science*. (2006).

36 Muller, C. & Usvyat, D. Incrementally Corrected Periodic Local MP2 Calculations: I. The Cohesive Energy of Molecular Crystals. *J Chem Theory Comput* **9**, 5590-5598 (2013).

37 Stoll, H. The correlation energy of crystalline silicon. *Chemical Physics Letters* **191**, 548-552, doi:http://dx.doi.org/10.1016/0009-2614(92)85587-Z (1992).

38 Stoll, H. On the correlation energy of graphite. *The Journal of Chemical Physics* **97**, 8449-8454, doi:doi:http://dx.doi.org/10.1063/1.463415 (1992).

39 Stoll, H. Correlation energy of diamond. *Physical Review B* **46**, 6700-6704 (1992).

40 Birkenheuer, U., Fulde, P. & Stoll, H. A Smplified Method for the Computation of Correlation Effects on the Band Structure of Semiconductors. *Theor Chem Acta* **116**, 398-403, doi:10.1007/s00214-006-0091-7 (2006).

41 Huang, C., Pavone, M. & Carter, E. A. Quantum mechanical embedding theory based on a unique embedding potential. *The Journal of Chemical Physics* **134** (2011).

42 CRYSTAL09 User's Manual (University of Torino, Turin, Italy, 2009).

43 Werner, H.-J. & Schütz, M. *J Chem Phys* **135** (2011).